Characterization of regular periodic surface structure by multi-pulse laser irradiation of a Zinc target

Ming Chen (陈 明)[1,2*], Xiangdong Liu (刘向东)[1,2], Yuehua Liu (刘月华)[1,2], and Mingwen Zhao (赵明文)[1,2]

[1] *School of Physics, Shandong University, Jinan 250100, China*

[2] *State Key Laboratory of Crystal Materials, Shandong University, Jinan 250100, China*

[*] *Corresponding author: chenming@sdu.edu.cn*

Received October 26, 2011; accepted November 24, 2011; posted online February 17, 2011

The circular-like sidewall and trench around the periphery of the crater are obtained on Zinc metal surface subjected to fewer than 200 cumulative pulses laser ablation. These patterns can be attributed to the higher secondary heating by regular plasma spherical pressure. The 600 pulses laser ablation, however, results in the formation of undesirable bulk wrinkles of super-heated liquid at the side of the trench. These features may be applied in micro-manufacturing of high localizability and selectivity using laser zone texturing.

OCIS codes: 140.0140, 180.0180, 300.0300.

doi: 10.3788/COL201210.051402.

The use of pulsed laser ablation has been established for high-precision drilling or micromachining of materials, such as metals, ceramics, polymers, and semiconductors[1−6]. It carries certain advantages such as, no mask needed, high efficiency, selectivity, and localizability. In previous studies, a lot of work has been focused on the central holes formed on the substrate, which have a variety of applications, such as grapheme fabrication on the nickel[1] and organic light emitting diode (OLED) based on laser transfer[3]. However, the mechanisms of regular and deformed patterns at the outside region of the molten area have not been thoroughly understood, partly because the inevitable vaporizing and recasting of material results in complicated patterns around the molten area, even with femtosecond laser ablation[3−7]. In the ablation process of multi-pulses laser with high intensity, the interactions between subsequent laser beams and plasma, secondary heating of the substrate, and higher shear stress frequently occur in the region around the periphery of the crater.

The physical process and mechanisms of the formation of regular and deformed patterns around the periphery are valuable to understand and improve pulsed laser ablation, which is expected to play an important role in the process of "laser zone texturing"[5]. Laser texturing relies on the hydrodynamic redistribution of the molten region produced by inhomogeneous heating, which is a particularly powerful method for creating subtle changes in morphology with satisfactory control over the lateral and vertical dimensions of the surface[5]. Therefore, the study of the mechanisms involved in the formation of regular periodic structure at the edge of the molten area is absolutely necessary.

Zinc metal is a sensitive test of surface damage under multi-pulses laser treatment due to its low melting point. In this letter, detailed scanning electron microscopy combined with alpha- step profile measurement of bombarded areas in ablated Zinc (Zn) was conducted. The variation of the plasma parameter created by subsequent laser beam was used to provide insight for the characterization of regular and deformed patterns around the periphery of crater. We may offer reasonable implications on the localizability and selectivity of micro- and macro-components manufacturing using laser zone texturing.

A laser beam from a Nd:YAG laser (Quanta Ray, Spectra Physics) was focused through a quartz lens (50 mm focal length) on a well-polished and pure (99.99%) zinc metal target located inside a vacuum chamber (10^{-2} Torr). In this experiment, the 1 064-nm laser beam fixed at 1.45 GW/cm^2 was operated in multi-transverse electro magnetic (TEM) modes with pulse length of 10 ns and a 10-Hz repetition. The bombarded areas on the target were examined using a Field Emission Scanning Electron Microscope (Hitachi High-Tech) operated at 15 kV and step profile measurement (Tencor 200 Alpha-step) after the laser shots. Optical emission spectroscopy was used to study the evolution of expanding plasma, and the emission spectra was detected by a time-gated (gate width of 2 ns) and intensified charge-coupled device (ICCD) (Andor Technology) at different time intervals.

The typical surface profile of a bombarded area on the Zn target produced by 200 cumulative pulses ablation was characterized by an scanning electron microscopy (SEM) micrograph, as shown in Fig. 1. The SEM micrograph (Fig. 1(a)) shows that re-depositions of super-heated material with wave ridges morphology were formed in the central region of the molten area. Moreover, its high resolution image (Fig. 1(b)) indicates that numerous small pits or grains of droplets were formed on the ridges. These results can be explained during the process of cooling or reforming of molten material using the mechanisms proposed in previous literatures[2,5−7], such as interference contribution, inhomogeneous temperatures, surface tension, and molten liquid oscillation.

Some regular pronounced removal and recast of materials that resulted in the formation of circular wave-like sidewall (shallow rim) and trench (deep groove) at the edge of the molten area were observed along the periphery, as shown in Fig. 1(a). In addition, molten droplets with strip-line shapes were formed at the bottom of the trench, as shown in Fig. 1(c). The radius of the sidewall

in Fig. 1(a) was approximately 500 μm, and the height of the sidewall was about 47 μm over the original surface, whereas the maximum depth and diameter of the trench around the melt pool are 64 and 110 μm, respectively. The higher vaporization and plasma spherical pressure around the periphery of bombarded area should be taken into consideration in explaining the formation of the regular sidewall and trench. The vaporization and plasma evolution occurred within a very short time period after the start of the laser pulse, and the interaction of the spherical shock wave of the plasma with molten material is responsible for the higher secondary heating at the periphery of the molten area due to inverse bremsstrahlung and photoionization. This process increases the mechanical load applied on the molten material around the crater, thus, more material will be preferentially removed in the path of a circular track. The circular-like pressure suddenly dropped and decayed quickly toward to the edge at the end of the pulses, which cooled down the super-heated liquid. The vaporization and recast of Zn occurred in the same circular track after the end of each laser pulse following the correct number of applied ablation pulses, which formed a circular- like sidewall and trench around the periphery of the central crater, as shown in Fig. 1(c).

The surface morphology of Zn sample significantly changed when the applied ablation pulse was further increased to 600 times. The low-resolution image in Fig. 2(a) illustrates periodically wavy structural features in the central crater, which is consistent with the description in Fig. 1(b), whereas the high-resolution image in Fig. 2(b) shows extensive re-deposition of super-heated liquid or bulk wrinkles in the sidewall, as well as deformation or irregular magnitude of trench, which is even

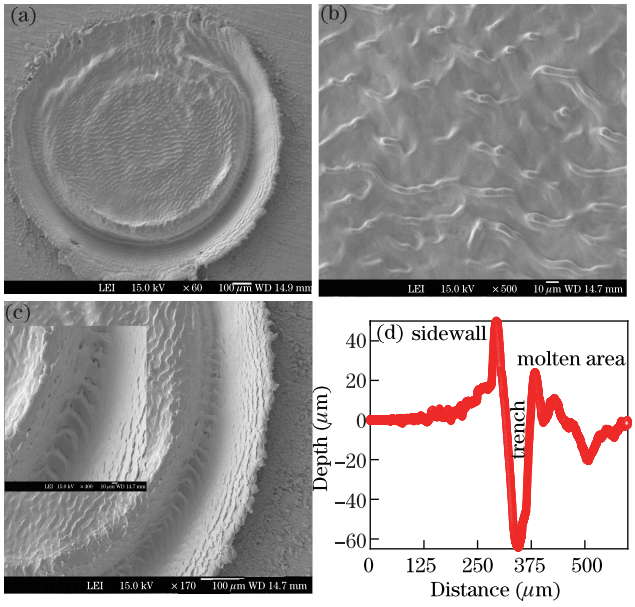

Fig. 1. Typical image of post-ablation on the Zn metal formed by 200 pulses laser with a power density of 1.45 GW/cm^2 in vacuum condition. (a) Low and (b, c) high magnification images illustrate the period-wavy structural feature in central crater and nearly regular circular-like sidewall and trench at edge of melt pool area. The depth and diameter of the sidewall and trench are given in (d), which are measured using the step profile method.

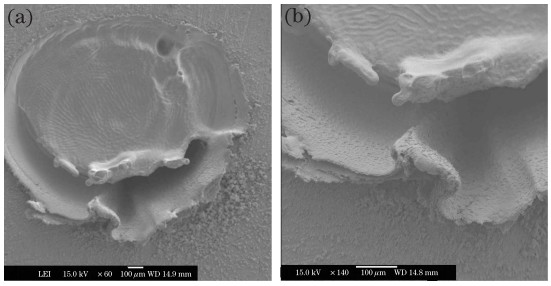

Fig. 2. (a) Overall image taken from the ablated spot on Zn target after 600 pulses laser beam. The bulk wrinkles in the sidewall and deformation or irregular magnitude of trench are observed in the corresponding high-magnification images (b).

more apparent compared with Figs. 1(b) and (c).

Some remarkable differences between the observed patterns under 200- and 600-laser ablated Zn metal were observed. Based on our experimental data, it can be concluded that these differences may be partly caused by a significant absorption enhancement in the process of subsequent laser pulses interaction with a structurally modified surface[7], as well as the non-linear interaction with plasma. Therefore, it is worthwhile to study the variation of plasma parameter created by subsequent laser pulses, which strongly depends on laser-material interaction.

In previous studies, plasma parameters such as electron temperature (T_e) and density (N_e)[8−11] can be obtained with reasonable accuracy from either the well-known Boltzmann plot method or the Stark broadening of well-isolated lines based on plasma emission spectroscopy. The approximate excitability temperature was determined by the Boltzmann plot method[8−11] under the assumption of local thermodynamic equilibrium (LTE).

$$\ln(I\lambda/Ag_m) = -E_m/kT_e + B, \tag{1}$$

where I, λ, and A refer to the relative integrated intensity, wavelength, and spontaneous emission rate, respectively. g_m is the statistical weight factor for the excited state, E_m is the energy of the excited state, k is the Boltzmann constant, and B is a constant parameter for all ion lines considered. In the current study, five spectral lines of Zn atoms at 330.26, 334.50, 472.21, 481.05, and 636.2 nm were selected to evaluate electron temperature. The emission lines from Zn ions were collected at a fixed distance of 3 mm from target surface, and spectroscopic constants of these spectral lines were obtained from Ref. [12].

In addition, the full-width at half-maximum ($\Delta\lambda_{1/2}$) of Stark broadened profile from well-isolated spectral lines is related with the electron density N_e in plasma through this relationship[8−13]:

$$N_e = \left(\frac{\Delta\lambda_{1/2}}{2W}\right) \times 10^{16}\ (\mathrm{cm}^{-3}), \tag{2}$$

where W is an electron impact parameter, which is weakly related to different temperatures. The Stark-broadened FWHM of Zn atoms at 334.50 nm was used to determine the electron density for the evaluation of N_e. $W = 0.0327$ nm was used with the increase of temperature in the range from 40 000 K to 80 000 K.

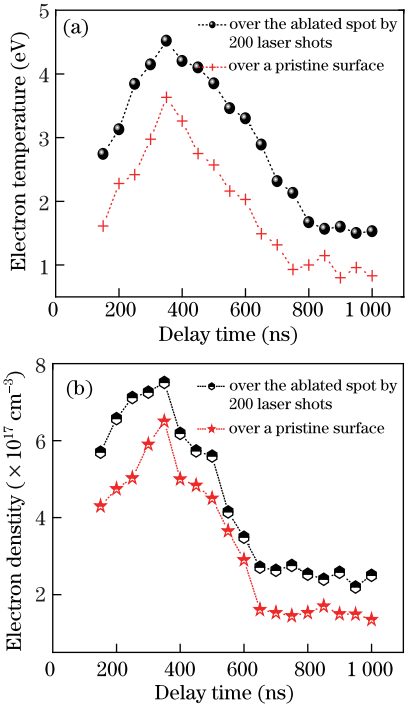

Fig. 3. Temporal evolution of electron temperature (a) and density (b) of expanding plasma created by subsequent laser pulses over a pristine surface and the ablated spot by 200 pulses laser ablation.

After 200 laser pulses ablating Zn targets, the ablated spot and another pristine target were irradiated using a train of laser pulses of the same fluence rate to induce plasma spectroscopy. Figures 3(a) and (b) illustrate the temporal evolution of electron temperature and density of plasma by subsequent laser pulses. The curves of electron temperature and density-versus-delay time show a very similar profile under two different experiment conditions. The values of electron temperature and density in a stage of expanding plasma created over the ablated spot were significantly higher than those over a smooth surface.

In a representative sample, at the delay time region of about 350 ns, the electron temperatures of plasma generated over a spot ablated by 200 laser shots and a pristine surface were calculated to be 4.52 and 3.63 eV, respectively at the delay time region of about 350 ns. These results clearly reveal that hotter and denser plasma can be obtained by increasing the number of applied ablation pulses. This phenomenon is attributed to the additional absorption enhancement of subsequent laser beams interacting with a structurally modified surface[7,14,15]. In this case, material will be significantly removed, resulting in the formation of a deeper trench in substrate surface. Furthermore, the interaction of hotter plasma with ejected molten material and higher shear stresses exaggerate the size of the recast layer. Meanwhile, dynamic denser plasma is initiated by further increasing the number of applied ablation pulses that will cause interference with subsequent laser beams, thereby allowing the laser beam to be deflected from the regular interaction zone. The non-linear interaction of high intensity laser beam with hotter and denser plasma may be responsible for the formation of undesirable bulk wrinkles of super-heated liquid in the sidewall, and the deformation of irregular magnitude of the trench.

In conclusion, we report on the formation of circular-like sidewall and trench around the periphery of the crater created by cumulative 200-ns pulses laser ablation of Zn metal. Non-linear interactions of subsequent laser with hotter and denser plasma result in undesirable bulk wrinkles of super-heated liquid observed in the sidewall caused by 600 laser beams. This remarkable difference may be explained by the interaction of subsequent laser pulses with a structurally modified surface. If one can properly control the higher secondary heating caused by plasma spherical pressure within 200 laser pulses with high intensity. These desirable features may be applied in micro-manufacturing with high localizability and selectivity through laser zone texturing. The vaporization of Zn material will be effectively moderated to achieve a regular-patterned sidewall and trench around the periphery of the crater.

This work was supported by the National Natural Science Foundation of China under Grant Nos. 11075097 and 10974119.

References

1. 1. J. B. Park, W. Xiong, Y. Gao, M. Qian, Z. Q. Xie, M. Mitchell, Y. S. Zhou, G. H. Han, L. Jiang, and Y. F. Lu, Appl. Phys. Lett. **98,** 123109 (2011).
2. D. Bouilly, D. Perez, and L. J. Lewis, Phys. Rev. B **76,** 184119 (2007).
3. S. H. Ko, H. Pan, S. G. Ryu, N. Misra, C. P. Grigoropoulos, and H. K. Park, Appl. Phys. Lett. **93,** 151110 (2008).
4. C. H. Lin, Z. H. Rao, L. Jiang, W. J. Tsai, P. H. Wu, C. W. Chien, S. J. Chen, and H. L. Tsai, Opt. Lett. **35,** 2490 (2010).
5. T. Schwarz-Selinger, and D. G. Cahill, Phys. Rev. B **64,** 155323 (2001).
6. I. Avrutsky, D. G. Georgiev, D. Frankstein, and G. Auner, Appl. Phys. Lett. **84,** 2391 (2004).
7. A. Y. Vorobyev, and C. Guo, Phys. Rev. B **72,** 195422 (2005).
8. M. Chen, X. Liu, M. Zhao, and Y. Sun, Opt. Lett. **34,** 2682 (2009).
9. M. Chen, X. Liu, M. Zhao, C. Chen, and B. Man, Phys. Rev. E **80,** 016405 (2009).
10. J. Siegel, G. Epurescu, A. Perea, F. J. Gordillo-Vázquez, J. Gonzalo, and. C. N. Afonso, Opt. Lett. **29,** 2228 (2004).
11. F. J. Gordillo-vazquez, A. Perea, J. A. Chaos, J. Gonzalo, and C. N. Afonso, Appl. Phys. Lett. **78,** 7 (2001).
12. W. L. Wiese and G. A. Martin, *Atomic Transition Probabilities* (National Stand, Washington, 1969).
13. G. Bekfi, *Principles of Laser Plasmas* (New York, Wiley, 1976).
14. I. I. Beilis, Appl. Phys. Lett. **89,** 091503 (2006).
15. I. I. Beilis, Laser and Particle Beams **25,** 53 (2007).